

Theoretical study of dark resonances in micro-metric thin cells

H. Failache,* L. Lenci, and A. Lezama

*Instituto de Física, Facultad de Ingeniería, Universidad de la República,
J. Herrera y Reissig 565, 11200 Montevideo, Uruguay*

D. Bloch and M. Ducloy

*Laboratoire de Physique des Lasers, UMR 7538 du CNRS, Institut Galilée,
Université Paris 13, 99 av. J.-B. Clément, 93430 Villetaneuse, France*

(Dated: October 28, 2018)

We investigate theoretically dark resonance spectroscopy for a dilute atomic vapor confined in a thin (micro-metric) cell. We identify the physical parameters characterizing the spectra and study their influence. We focus on a Hanle-type situation, with an optical irradiation under normal incidence and resonant with the atomic transition. The dark resonance spectrum is predicted to combine broad wings with a sharp maximum at line-center, that can be singled out when detecting a derivative of the dark resonance spectrum. This narrow signal derivative, shown to broaden only sub-linearly with the cell length, is a signature of the contribution of atoms slow enough to fly between the cell windows in a time as long as the characteristic ground state optical pumping time. We suggest that this dark resonance spectroscopy in micro-metric thin cells could be a suitable tool for probing the effective velocity distribution in the thin cell arising from the atomic desorption processes, and notably to identify the limiting factors affecting desorption under a grazing incidence.

PACS numbers: 39.30.+W 32.70.Jz 42.62.Fi 42.65.-K

I. INTRODUCTION

Large attention has been devoted during the last years to coherently prepared atomic media. Coherent Population Trapping (CPT), Electromagnetically Induced Transparency (EIT), Electromagnetically Induced Absorption (EIA), sub-recoil laser cooling, lasing without inversion, strong dispersive media, fast and slow light are some examples of physical phenomena resulting from the interaction of light fields with coherently prepared media.

EIT is a nonlinear optical effect typically observed in a Λ -type three-level atomic system interacting with two electromagnetic fields. The significant reduction of the medium absorption, occurring near the Raman resonance condition, can be understood as the consequence of the existence of a coherent superposition of ground levels (a dark state) which is not coupled to the excited state by the fields. Atoms falling in this dark state stay trapped as the electromagnetic field is unable to excite them. Transparency is then induced as a consequence of the optical pumping of the atomic system into this dark state. In consequence, EIT resonances are commonly designated as dark resonances as we will do in the following. The width of the dark resonance when the Raman detuning is varied is essentially determined by the coherence loss rate of the lower (ground) states. In closed Λ systems, the optical pumping rate to the dark state defines a lower limit for the resonance width [1]. However a quite different behavior is observed for open

systems, where the lower limit of the resonance width (in the absence of other dephasing processes) appears to be only determined by the interaction time of the atoms with the laser radiation [2]. For an atomic vapor inside a macroscopic cell the interaction time is essentially determined by the time of flight of atoms through the laser beam. A buffer gas, resulting in a diffusive atomic motion, is frequently used in order to largely increase such a time. Another approach consists in avoiding the atom coherence loss at the walls of the container by using a paraffin coating. In practice, other factors such as collisions or magnetic field inhomogeneities can result in additional ground state decoherence. Dark resonance spectra in macroscopic cells can be extremely narrow, spectral widths smaller than 50 Hz have been measured in buffered cm-long cells [3, 4].

Considerable attention is presently directed to the use of miniaturized atomic cells as practical metrological standards. Dark resonances in miniaturized cells have been used as compact atomic frequency references [5, 6] and compact magnetometers [7]. However, in order to obtain narrow resonances with such miniaturized cells, large buffer gas pressures must be used to provide a small enough atomic diffusion lengths. The use of miniaturized buffer gas cells has the drawback that the dark resonance linewidth grows very fast when the cell characteristic dimension L is reduced ($\text{width} \propto L^{-2}$ [8]). The spectroscopic properties of small size cells can be considerably different than those of larger ones if the cell dimensions are small compared to the mean free path of the atoms in the vapor. An example of this is given by the linear absorption spectrum of an atomic gas with 1D confinement between two close parallel windows obtained in a thin cell. In this case the atomic

*Electronic address: heraclio@fing.edu.uy

sample becomes anisotropic since atoms flying parallel to the windows interact with light during a much larger time than those flying perpendicular to the windows. Such an anisotropy is responsible for the observation of sub-Doppler features in the spectrum [9, 10].

Dilute atomic vapor cells, in which the atomic trajectories are from wall-to-wall, can be classified in three different classes depending on the interaction time of an atom flying at the mean thermal velocity \bar{v} . “Long” cells are those where the average time of flight exceeds the longest characteristic time of the atomic evolution generally given by an optical pumping time τ_p , i.e. $L \gg \bar{v}\tau_p$. In such cells, an atom departing from one wall reaches a steady state regime before hitting the opposite cell wall. Intermediate cells, designated as “micro-metric” cells [11] are those for which $\bar{v}\tau_p \gtrsim L \gtrsim \frac{\bar{v}}{\Gamma}$ (Γ^{-1} : excited state lifetime). In these cells the atom-light interaction time is long compared to the excited state decay which means that several absorption-emission cycles can take place. However, the optical pumping efficiency is strongly dependent on the atomic velocity and only the slowest atoms may approach a steady state. Finally, nanometric cells are those for which $L \lesssim \frac{\bar{v}}{\Gamma}$ which means that the optical relaxation can be neglected during the atomic flight, the regime is a coherent build-up of the atomic excitation for those cells whose length is typically shorter than the optical wavelength.

Micro-metric thin cells were used in optical pumping experiments with a single irradiating beam at normal incidence. The strong dependence of the interaction time with the atomic velocity results in the observation of Doppler free absorption spectral lines [9]. Nano-metric cells have been used to observe the enhancement of the coherent transient atomic response due to Dicke narrowing, and to study long-range atom-wall interaction [12, 13]. Recently, a merging between the domain of EIT in miniaturized cells and spectroscopy in anisotropic thin cells, has led to the observation of dark resonances in micro-metric thin cells [6, 14, 15] and even in nano-metric thin cells [16, 17]. It is the purpose of the present paper to describe theoretically the main spectroscopic features of dark resonances in micro-metric thin cells [18, 19, 20, 21], with an emphasis on the contribution of slow atoms.

II. THEORETICAL STUDY

A. Atomic model

We have chosen to study the properties of dark resonances in micro-metric cells through the analysis of a scheme applicable to the experimental situation of an atomic transition with a lower level with total angular momentum $F = 1$ and an excited state with angular momentum $F' = 0$ interacting with a single linearly polarized optical field propagating along the quantization

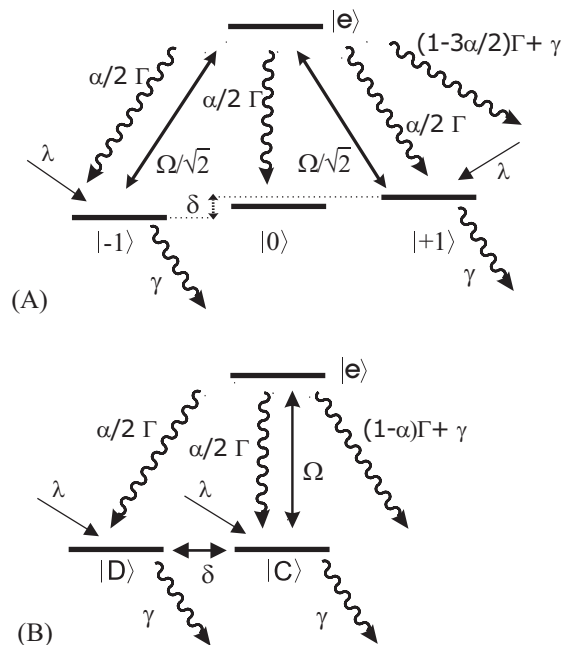


FIG. 1: A) Atomic model, transition $F = 1 \rightarrow F' = 0$ B) Elementary 3-level atomic model in the base $|C\rangle$, $|D\rangle$.

axis. With the incident field expanded into the components of the two eigen circular polarization components, this system constitutes a realization of a Λ system (see Fig. 1.A). The Raman detuning can be easily tuned with the help of a magnetic field collinear with the light beam. Similar configurations, usually designated as Hanle/CPT schemes, have been used in many EIT experiments [1, 2, 22, 23, 24]. The system is open since the atoms can decay from the excited state into the $|F = 1, m_F = 0\rangle$ or into external states. The choice of this configuration is motivated by its large symmetry (equal atom-field coupling and decay rates on the two arms of the Λ system) which allows to simplify the discussion due to a reduction in the number of independent parameters. Although our study is based on a specific case, our conclusions can be extended to the general case of an asymmetric Λ system.

The dynamics of the atomic system can be conveniently analyzed in the basis presented in Fig. 1.B where the lower states are the dark $|D\rangle \equiv \frac{1}{\sqrt{2}}(|1\rangle - |-1\rangle)$ and coupled $|C\rangle \equiv \frac{1}{\sqrt{2}}(|1\rangle + |-1\rangle)$ states [25, 26]. The optical fields couple the $|e\rangle$ and $|C\rangle$ states with the Rabi frequency Ω . For nonzero Raman detuning δ (corresponding to twice the Zeeman splitting introduced by the magnetic field) the $|D\rangle$ and $|C\rangle$ states are coupled. Population losses to external levels (including the $|F = 1, m_F = 0\rangle$ level in the precise case of a $|F = 1\rangle \leftrightarrow |F = 0\rangle$ transition), are described by a rate $(1-\alpha)\Gamma$, with Γ the optical width of the transition and α a branching ratio. The case of a closed system corresponds to $\alpha = 1$. Aside from a possible population loss -controlled by the parameter $(1 - \alpha)$ - a phenomenological decay rate γ is introduced

in the model to mimic the experimental conditions (finite beam diameter, field inhomogeneities, etc.) that set a lower limit to the lower level decoherence rate [1]. The arrival of fresh atoms to the system (essentially those leaving from the cell walls) is represented by constant and equal repumping terms (λ) for the lower levels. If the atomic density matrix is normalized to unity, we have $2\lambda = \gamma$. The Bloch equations describing the atom-field interaction in the $|e\rangle$, $|C\rangle$ basis (in the rotating wave approximation) are [22],

$$\dot{\sigma}_{DD} = \alpha \frac{\Gamma}{2} \sigma_{ee} + \delta \text{Im} \sigma_{DC} - \gamma \sigma_{DD} + \lambda \quad (1a)$$

$$\dot{\sigma}_{CC} = \alpha \frac{\Gamma}{2} \sigma_{ee} - \delta \text{Im} \sigma_{DC} + 2\Omega \text{Im} \sigma_{eC} - \gamma \sigma_{CC} + \lambda \quad (1b)$$

$$\dot{\sigma}_{ee} = -\Gamma \sigma_{ee} - 2\Omega \text{Im} \sigma_{eC} - \gamma \sigma_{ee} \quad (1c)$$

$$\dot{\sigma}_{eD} = -\left(\frac{\Gamma}{2} - i\Delta\right) \sigma_{eD} - i\frac{\delta}{2} \sigma_{eC} - i\Omega \sigma_{CD} - \gamma \sigma_{eD} \quad (1d)$$

$$\dot{\sigma}_{eC} = -\left(\frac{\Gamma}{2} - i\Delta\right) \sigma_{eC} - i\frac{\delta}{2} \sigma_{eD} - i\Omega(\sigma_{CC} - \sigma_{ee}) - \gamma \sigma_{eC} \quad (1e)$$

$$\dot{\sigma}_{DC} = i\frac{\delta}{2}(\sigma_{CC} - \sigma_{DD}) + i\Omega \sigma_{De} - \gamma \sigma_{DC} \quad (1f)$$

where $\Delta = \delta\omega - kv_z$ is the optical detuning, v_z being the component of the atomic velocity perpendicular to the cell window, k the amplitude of the wave vector characterizing the incident irradiation and $\delta\omega$ the detuning of the laser with respect to the optical transition for an atom at rest. The steady state solution of Bloch equations (Eqs. 1) is not useful in the present case because the atoms contributing to the coherence resonance are essentially in transient regime of interaction. In consequence, the Bloch equations should be integrated to obtain the atomic density matrix $\sigma(t)$ as a function of the interaction time which is the time elapsed after the atom has left a cell window. The light intensity absorbed by the atomic vapor in a thin cell of thickness L is given by [10, 27]:

$$\Delta I = \kappa \Omega \int_{-\infty}^{\infty} \int_0^L W(v_z) \text{Im} \sigma_{eC}(z, v_z) dz dv_z \quad (2)$$

where z is the distance perpendicular to the cell window (along laser propagation) and κ is a coefficient proportional to the atomic density (an optically thin atomic medium will be assumed along this article). In Eq. 2 the interaction time does not appear explicitly; z is related to t through $z = v_z t$, for the atoms leaving the cell

surface at $z = 0$ and $z - L = v_z t$ for atoms leaving the cell surface at $z = L$. $W(v_z)$ is the velocity distribution function assumed to be the Maxwell-Boltzmann (M-B) distribution. Note that when the laser is taken at resonance with the optical transition ($\delta\omega = 0$), as will be assumed along this article except in section II E, the contribution of positive and negative velocities in Eq. 2 are equal. Such an assumption ensures that the light is resonant with the atoms with small velocity component v_z in the direction perpendicular to the cell windows. This assumption does not represent a strong experimental restriction since it is enough for the laser detuning to satisfy $\delta\omega < \Gamma$, as will be discussed in section II E. Multiple reflections of the laser beam at the cell windows modify the atomic absorption due to a Fabry-Perot effect. Such an effect is small if the cell length L is longer than the laser wavelength and will be neglected here [28]. Boundary effects, such as the finite light beam diameter, are assumed to be taken into account by the relaxation rate γ .

B. Characteristic parameters and lineshape predictions

We consider here the simple situation $\gamma = \lambda = 0$ (i.e. the loss of population and arrival of fresh atoms are neglected on the time scale involved in the atom-light interaction; the role of γ is considered in IID). From the analytic expression of the eigenvalues of the matrix associated to the first order differential equations system (Eq.1) it is possible to identify dimensionless parameters characterizing the dark resonance spectra in a thin cell. The corresponding discussion together with the numerical verification is deferred to the Appendix. We find that the atomic response, as a function of the Raman detuning, depends on the cell length L and the light intensity through the dimensionless characteristic parameter

$$\phi = \frac{\Omega^2 k L}{\Gamma^2} \quad (3a)$$

with

$$\frac{\Omega^2}{\Gamma} = \gamma_p \quad (3b)$$

where γ_p is the optical pumping rate from the $|C\rangle$ state. Note that $\gamma_p L$ represents the maximal velocity allowing an atom to hit the opposite wall after an efficient pumping, while $\frac{\Gamma}{k}$ is the velocity width for optical processes of velocity selection. The parameter ϕ , already noticed as a characteristic one in single beam optical pumping experiments [9], appears to be the ratio between the specific kind of velocity "selection", as allowed by the optical pumping, over the classical optical velocity selection. The atomic response depends also on the branching ratio α and the dimensionless Raman detuning $\frac{\delta}{\gamma_p}$.

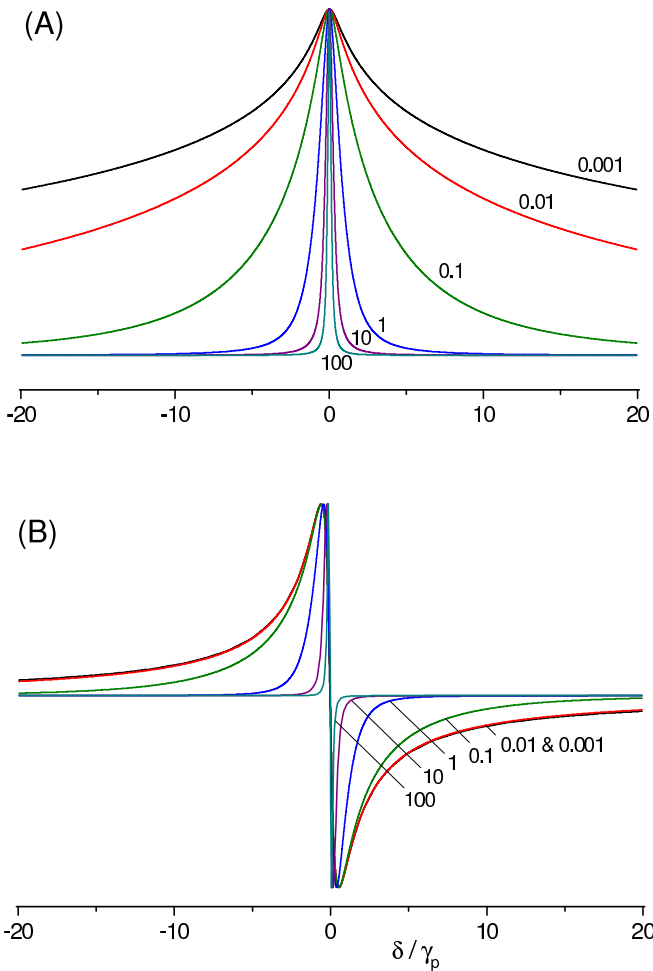


FIG. 2: (Color online) A) Dark resonance spectra for different values of the parameter ϕ ($\Omega = 0.01\Gamma$, $\alpha = 0.7$, $\lambda = \gamma = 0$). For the purpose of line-shape comparison, the amplitude of spectra are normalized. (The vertical axis corresponds to transmission). B) Derivative with respect to the Raman detuning of the spectra shown in A). The corresponding spectrum amplitudes A , relative to the one for $\phi = 1$, are: A) $A_{0.001} = 1.0 \times 10^{-5}$, $A_{0.01} = 7.5 \times 10^{-4}$, $A_{0.1} = 3.8 \times 10^{-2}$, $A_1 = 1$, $A_{10} = 9.9$, $A_{100} = 56.4$; B) $A_{pp0.001} = 1.4 \times 10^{-6}$, $A_{pp0.01} = 1.4 \times 10^{-4}$, $A_{pp0.1} = 1.4 \times 10^{-2}$, $A_{pp1} = 1$, $A_{pp10} = 28.6$, $A_{pp100} = 367$.

As expected it is the optical pumping rate γ_p and not the strength of the optical coupling Ω , that determines the relevant time-scale of the atomic evolution. All over the paper we will assume $\Omega \ll \Gamma$. This is because the interesting effects for the dark resonance should not be altered by the saturation and broadening of the optical transition. Hence, the transient effects on the optical coherence, at the heart of nanometric cell behavior, can be neglected. This also implies that large ϕ values are associated to relatively long cell lengths.

Fig. 2 shows the dark resonance spectra for different values of the characteristic parameter ϕ , the other parameters being kept constant. In Fig. 2 and generally all along this work, the dark resonance spectrum is isolated from

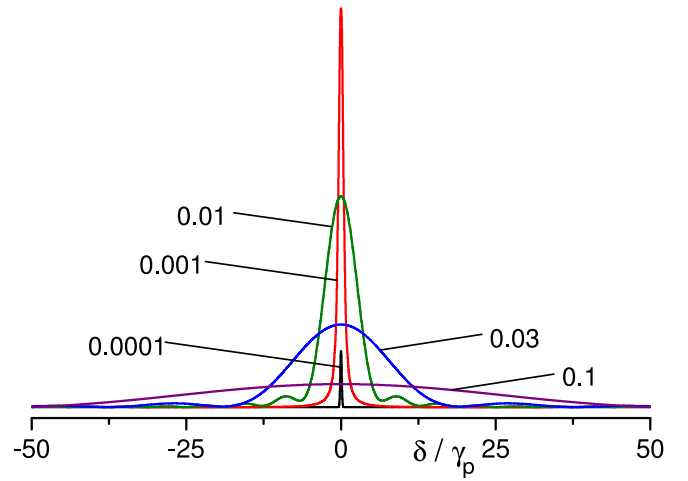


FIG. 3: (Color online) Contribution of different velocities v_z to a dark resonance spectrum. The vertical axis corresponds to transmission. The choice of parameters $\phi = 0.01$, $\alpha = 0.7$, $\lambda = \gamma = 0$ corresponds to a relatively broad spectrum. The figures on each curve correspond to the velocity in $\frac{\Gamma}{k}$ unit.

the spectrum obtained from Eq.2 subtracting the linear absorption and the single beam optical pumping spectra [9] broad background calculated separately.

The shape of the dark resonance spectra for small values of ϕ is characterized by slowly decreasing wings and a sharp peak at $\delta = 0$. Although the width and shape of the spectra considerably evolve with the parameter ϕ , one notes a persistent singularity at line center. Such a sharp central feature is better seen (Fig. 2.B) when considering the derivative of the spectrum with respect to the Raman detuning, as can be practically obtained through a demodulation of a modulated Zeeman structure. In the following, we mostly concentrate on the analysis of this derivative of the spectrum.

Slow atoms, having long time of interaction, contribute to the coherent signal through narrow resonances while faster atoms essentially contribute to the broad wings of the coherent signal (see Fig. 3). Although slow atoms are rare, their contribution at line-center is of comparable importance to that of the more abundant fast atoms. Moreover, it is the narrower contribution of slow atoms that dominates the spectrum derivative. The detailed behavior of the resonances can be notably illustrated through the evolution of the peak-to-peak width Δ_{pp} of the derivative of the dark resonance spectra as a function of the dimensionless parameter ϕ (Fig. 4). In a more practical manner, Fig. 4 shows the influence of the cell thickness L . Indeed, ϕ is proportional to L , so that ϕ can be seen as a length ratio $\frac{L}{L_o}$ when a given Rabi frequency Ω is assumed (L_o is a characteristic length defined as $L_o \equiv \frac{\Gamma}{k\gamma_p}$, it represents the length above which the optically selected atoms with $|v_z| < \frac{\Gamma}{k}$ approach the steady-state relatively to the Raman coherence). Two different regimes can be distinguished according to $L \lesssim L_o$ or $L \gtrsim L_o$ (i.e. $\phi \lesssim 1$ or $\phi \gtrsim 1$). In addition, differences

between closed and open systems appear when $L \geq L_o$ (i.e. $\phi \geq 1$).

For the thinnest cells it can be seen that the spectral width reach a maximum $\Delta_{pp} \approx \gamma_p$. Such a maximal width is imposed by the interaction time, of the order of one pumping cycle γ_p^{-1} , required to reach a significant dark state preparation (in this regime ($\phi \lesssim 1$) every atom contributing to the spectrum is optically resonant and experiences the same γ_p). The fact that the width Δ_{pp} remains finite even for extremely thin cells, critically relies on the existence of atoms with arbitrarily slow longitudinal velocity. The existence of such slow atoms (as slow as the optically selected velocity $\frac{\Gamma}{k}$ times the arbitrary small ratio $\frac{L}{L_o}$), granted by the assumed M-B velocity distribution which has an almost flat dependence on v_z around $v_z = 0$, is actually questionable and discussed in III.

Increasing the cell thickness, the spectral width decreases for $L \gtrsim L_o$ (i.e. $\phi \gtrsim 1$). Various behaviors thus appears in Fig. 4 according to the atomic relaxation processes, including the closed or opened nature of the system. As was shown by Renzoni and coworkers [2], the population loss in open systems results in a continuous decrease of the dark resonance width with the interaction time. This narrowing is due to the fact that population losses increase with detuning. In consequence, it reduces the spectral wings with respect to the central feature (see Fig. 5).

Closed atomic systems should be analyzed differently as the dark resonance width in a closed system is determined by the pumping rate γ_p [1]. The spectral width Δ_{pp} experiences slight variations (of at most one order of magnitude) as a function of L between the upper and lower limits, both related to the pumping rate γ_p . The slight narrowing of the spectra observed for $L \gtrsim L_o$ ($\phi \gtrsim 1$) can be understood if one includes the contribution of atoms Doppler-detuned from resonance ($kv_z \gtrsim \Gamma$). In this regime, nonresonant atoms may have enough time to be optically pumped into the dark state. However, the optical pumping rate for these Doppler-detuned atoms is smaller than γ_p resulting in a narrower contribution to the dark resonance spectra as emphasized in the spectrum derivative. Although the contribution of a nonresonant atom is smaller compared to that of a resonant one, nonresonant atoms are abundant. The total number of atoms effectively contributing to the dark resonance spectrum increases with L up to a limit reached when all atomic velocities are involved. In our calculations (carried for a Doppler width $\Delta_D = 50\Gamma$) this limit is reached for $L \approx 10^6 L_o$.

In the numerical calculation we find that the narrowing of the dark resonance spectra for an open atomic system follows a L^{-S} ($L > L_o$) dependence on the cell thickness with $S \cong \frac{1}{3}$. Such a dependence suffers only slight variations with the branching ratio α (provided that $\alpha \lesssim 0.9$). Hence, the dark resonance spectral width in thin cells is less sensitive to confinement than an ideal spherical cell with diameter L for which the mean interaction time is

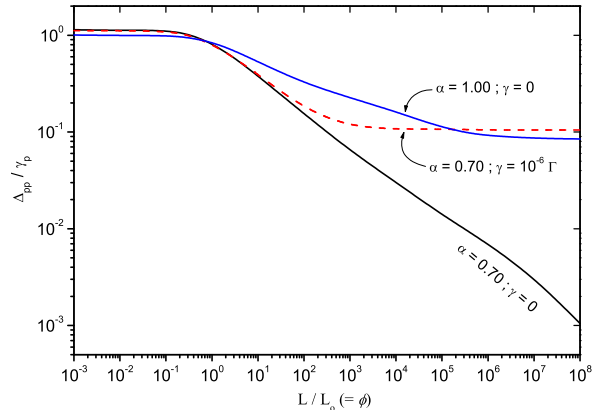


FIG. 4: (Color online) Peak-to-peak width of the derivative of the dark resonance spectra as a function of the cell thickness L ($\Omega = 0.01\Gamma$). Solid lines: $\lambda = \gamma = 0$ for an open system with $\alpha = 0.7$ and a closed system ($\alpha \equiv 1$). Dashed line: $\lambda = \gamma = 10^{-6}\Gamma$ ($\alpha = 0.7$).

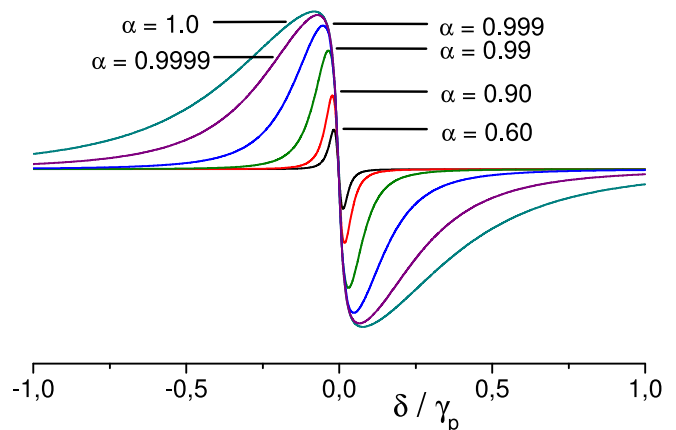


FIG. 5: (Color online) Influence of the population losses (determined by the parameter α) on the spectral narrowing for $\phi = 10^4$ and $\lambda = \gamma = 0$.

proportional to L and leads to the well known $\Delta_{pp} \propto L^{-1}$ dependence. Moreover, in the case of a spherical cell filled with a buffer gas, as a consequence of the diffusive motion of atoms, the interaction time is proportional to L^2 and the width of the dark resonance spectrum presents an L^{-2} dependence [8].

Alternately, the dependence on the dimensionless parameter ϕ can be discussed as a dependence on the irradiation laser intensity, as illustrated in Fig. 6. The apparent differences between Fig. 4 and Fig. 6 is related to the definition of the reduced coordinates for the vertical axis, as $\frac{\Delta_{pp}}{\gamma_p}$ now depends on Ω^2 . The two regimes $\phi < 1$ and $\phi > 1$ now appear as two regimes for the laser intensity $\Omega^2 \lesssim \Omega_o^2$ or $\Omega^2 \gtrsim \Omega_o^2$, where we introduce $\Omega_o^2 = \frac{\Gamma^2}{kL}$ ($\Omega^2 = \phi\Omega_o^2$) (Ω_o represents, for a given

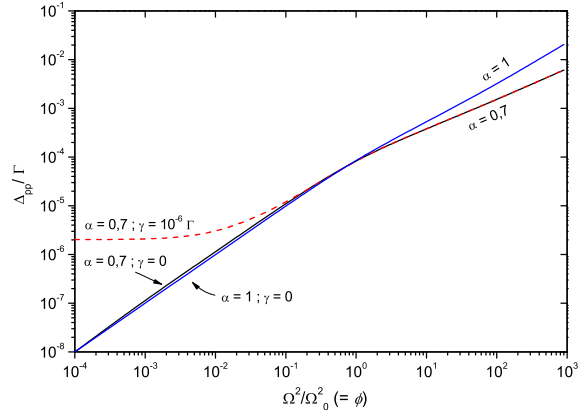


FIG. 6: (Color online) Peak-to-peak width of the derivative of the dark resonance spectra as a function of the laser intensity $\Omega^2(kL = 10000)$. Solid lines: $\lambda = \gamma = 0$ for an open system with $\alpha = 0.7$ and a closed system ($\alpha \equiv 1$). Dashed line: $\lambda = \gamma = 10^{-6}\Gamma$ ($\alpha = 0.7$).

cell thickness L , the Rabi frequency for which the whole optically selected zero-velocity class contributes to the coherence resonance). If $\Omega^2 \lesssim \Omega_o^2$ ($\phi \lesssim 1$) the atoms are essentially in a transient regime of interaction and the previously mentioned narrowing process in open systems is not effective [2]. In consequence, no essential difference is found between open or closed atomic systems, and the spectral width is determined by the pumping rate γ_p . In this case every atom contributing to the dark resonance spectrum is resonant with the optical field and affected by the same optical pumping rate γ_p . The spectral width Δ_{pp} is then proportional to γ_p (see Fig. 6). If $\Omega^2 \gtrsim \Omega_o^2$, for an open atomic system, the narrowing process already mentioned operates for every atom at resonance resulting in a slower increase of the spectral width with the laser intensity ($\Delta_{pp} = (\Omega^2)^{2S}$, $S \cong \frac{1}{3}$ for $\alpha \lesssim 0.9$). In the case of a closed atomic system, no narrowing process operates and the spectral width is determined by the pumping rate. The contribution of atoms detuned from the optical resonance (that have a smaller effective pumping rate γ_p) slows down the evolution of Δ_{pp} with the laser intensity. When all atomic velocities contribute to the coherence resonance (at $\Omega^2 \cong 10^6 \Omega_o^2$) the spectral width grows again proportionally to γ_p .

To understand to which extent the predicted narrow lineshapes can be effectively observed, it is needed to know also the evolution of the signal peak-to-peak amplitude A_{pp} with respect to the dimensionless parameter ϕ (Fig. 7). Again, one can discriminate two regimes $\phi \lesssim 1$ and $\phi \gtrsim 1$ and the respective evolution. For the first case the amplitude grows as ϕ^2 ; for $\phi \gtrsim 1$, it grows proportionally to ϕ . A deviation from this behavior is observed for an open system ($\alpha = 0.7$) around $\phi \gtrsim 10^6$, when the full Doppler velocity distribution contributes to the dark

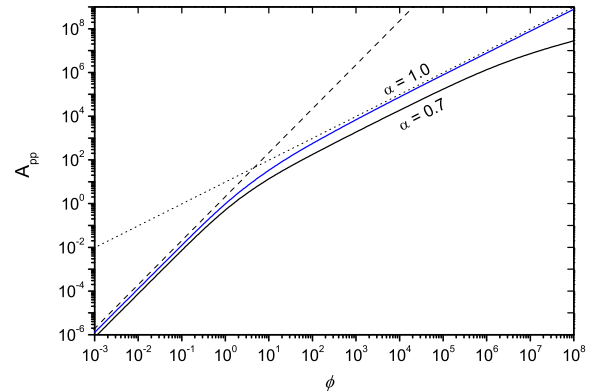


FIG. 7: (Color online) Theoretical peak-to-peak amplitude A_{pp} of the derivative of the dark resonance spectra calculated for different values of the parameter ϕ ($\Omega = 0.01\Gamma$, $\alpha = 0.7, 1.0$, $\lambda = \gamma = 0$). The values for A_{pp} were taken relative to its value at $\phi = 1$; $\alpha = 1$. The dashed line illustrates an asymptotic evolution proportional to ϕ^2 while the dotted line corresponds to a linear dependence on ϕ .

resonance spectrum. The peak-to-peak amplitude A_{pp} has a larger amplitude for a closed atomic system. This shows that the spectral narrowing of the dark resonance spectrum in an open system, that tends to increase the amplitude of the derivative, does not compensate for the population losses responsible for the narrowing mechanism [2].

C. Velocity selection.

The velocity selection performed by the coherent signal can be conveniently analyzed by considering the contribution of different velocity intervals to the dark resonance spectrum as given by the integral of Eq. 2. Following [10], the contribution of the various velocities to the coherent signal was analyzed by considering a partial integral for $|v_z| < \frac{\Delta_s}{k}$. Here again, two different situations should be considered depending on $\phi < 1$ or $\phi > 1$.

When $\phi < 1$ every atom contributing to the dark resonance spectrum is resonant with the optical transition. Fig. 8.A shows the evolution of the amplitude of the dark resonance spectrum as a function of Δ_s . It can be seen that the whole velocity interval $\frac{\Gamma}{k}$ ($\frac{\Delta_s}{\Gamma} = 1$) is essentially responsible for the observed signal. Almost no contribution to the amplitude of the spectra is due to velocities larger than $\frac{\Gamma}{k}$. However, if the derivative of the dark resonance spectrum is considered, the velocities contributing to this signal are well estimated by the smaller quantity $\phi \frac{\Gamma}{k}$ as can be seen in Fig. 8.B. Hence, almost no contribution to this spectrum arise from atoms out of the interval $\phi \frac{\Gamma}{k}$. The fact that the derivative of the spectrum is dom-

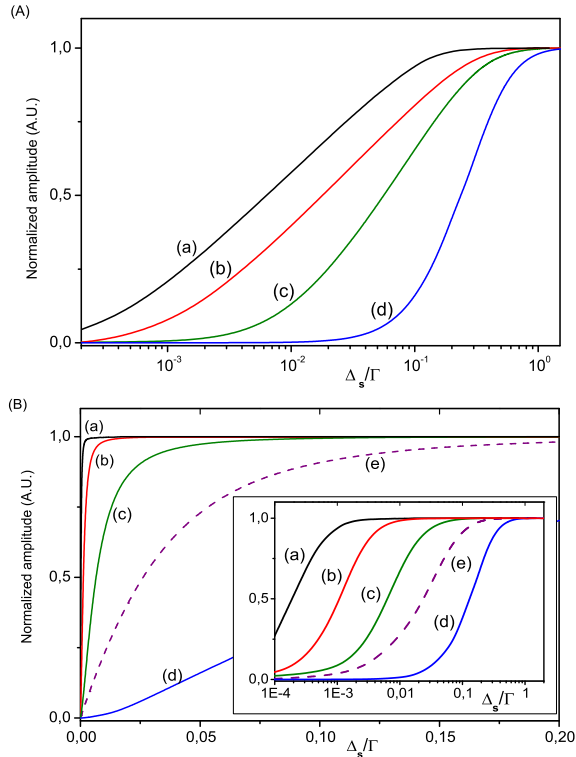


FIG. 8: (Color online) A) Partial velocity contribution to the direct (not derived) dark resonance spectra in a thin cell corresponding for (a) $\phi = 0.001$, $\gamma = 0$ (b) $\phi = 0.01$, $\gamma = 0$, (c) $\phi = 0.1$, $\gamma = 0$ and (d) $\phi = 1$, $\gamma = 0$, . B) Partial velocity contribution to the derivative of the dark resonance spectra in a thin cell for the curves (a-d) shown in A) and (e) $\phi = 0.01$, $\gamma L = 0.1 \frac{\Gamma}{k}$, $\frac{\gamma}{\gamma_p} = 10$. The data was normalized to the maximum amplitude.

inated (for $\phi < 1$) by the contribution of slow atoms with velocities $|v_z| < \frac{\Gamma}{k}$ (Fig. 3) is a signature of a "logarithmic singularity" [10, 29, 30] occurring when the contribution of large velocities to the direct spectrum decays as slowly as $\frac{1}{v_z}$.

For $\phi < 1$ we conclude that while, strictly speaking, every atom resonant with the optical transition (i.e. atoms in the velocity interval $\frac{\Gamma}{k}$) participates in the signal, the idea of a velocity selection remains a meaningful concept and the velocity range contributing to the spectra is well estimated by $\phi \frac{\Gamma}{k}$ as far as the spectrum derivative is concerned.

For $\phi > 1$, a fraction of the atoms that have enough time to contribute to the dark resonance spectrum before hitting the cell walls are actually fast enough to be Doppler-detuned from the frequency of the optical field. Such atoms effectively contribute to the dark resonance spectrum, as was already discussed in the preceding section, but the velocity interval participating in the spectra is largely over-estimated by $\phi \frac{\Gamma}{k}$. The full Doppler veloc-

ity distribution can however contribute to the spectrum for large enough values of ϕ (e.g. $\phi \cong 10^6$).

D. Role of the effective relaxation parameter γ .

As was previously mentioned, in order to account for the finite beam cross section as well as other possible sources of ground state decoherence, a phenomenological decay rate γ and a repumping process λ can be included in our model [see Fig. 1 and Eqs. (1)]. In consequence, the dark resonance spectrum is also characterized by the dimensionless coherence loss rate $\frac{\gamma}{\gamma_p}$ (see Appendix).

Considering that $\frac{\gamma}{\gamma_p} < 1$, the parameter γ introduces a lower limit in the width of the dark resonance spectrum for an open system as it is shown by the dashed line in Fig. 4. The build-up of the narrow resonance can be operated only during a mean time γ^{-1} , and as a consequence the limiting value for Δ_{pp} appearing for long enough cells depends on both rates γ and γ_p . Such a limiting value tends to $\Delta_{pp} = \gamma$ as the light intensity approaches zero.

When $\frac{\gamma}{\gamma_p} \geq 1$ (i.e. strong decoherence introduced by γ), the spectrum width is γ dependent for any cell length. In such a case, the mean atom-light interaction time is essentially limited by γ^{-1} and the velocity range that gives an effective contribution to the spectra can be estimated by γL , as shown at Fig. 8.B(e).

E. Effect of the laser detuning.

We here briefly address the situation of a nonzero detuning of the optical field ($\delta\omega \neq 0$). Once again the two different situations $\phi < 1$ and $\phi > 1$ should be distinguished as illustrated in Fig. 9. In the first one, a narrow contribution to the dark resonance spectrum is observable provided that the slowest atoms (corresponding to the velocity range $\phi \frac{\Gamma}{k}$ around zero) remains within the optically selected velocity class ($\delta\omega \leq \Gamma$). As $\delta\omega$ is increased the narrow contribution to the dark resonance spectrum decreases as a consequence of detuning (Fig. 9.A). Also, a broad structure appears in the dark resonance spectrum for $\delta\omega \gtrsim \Gamma$. This structure corresponds to optically selected fast atoms that have a small interaction time and thus a broader contribution to the spectra.

In the case $\phi > 1$, the range of velocities enabling an atom to contribute to the dark resonance spectrum increases. If $\frac{\delta\omega}{\Gamma} \lesssim \phi$ a fraction of this velocity range is optically selected and a narrow contribution to the spectrum is observed, as shown in Fig. 9.B (note in this figure that the amplitude of the dark resonance spectrum of the open system for $\frac{\delta\omega}{\Gamma} = 0$ is smaller than the one for $\frac{\delta\omega}{\Gamma} = 1$ due to population losses that are

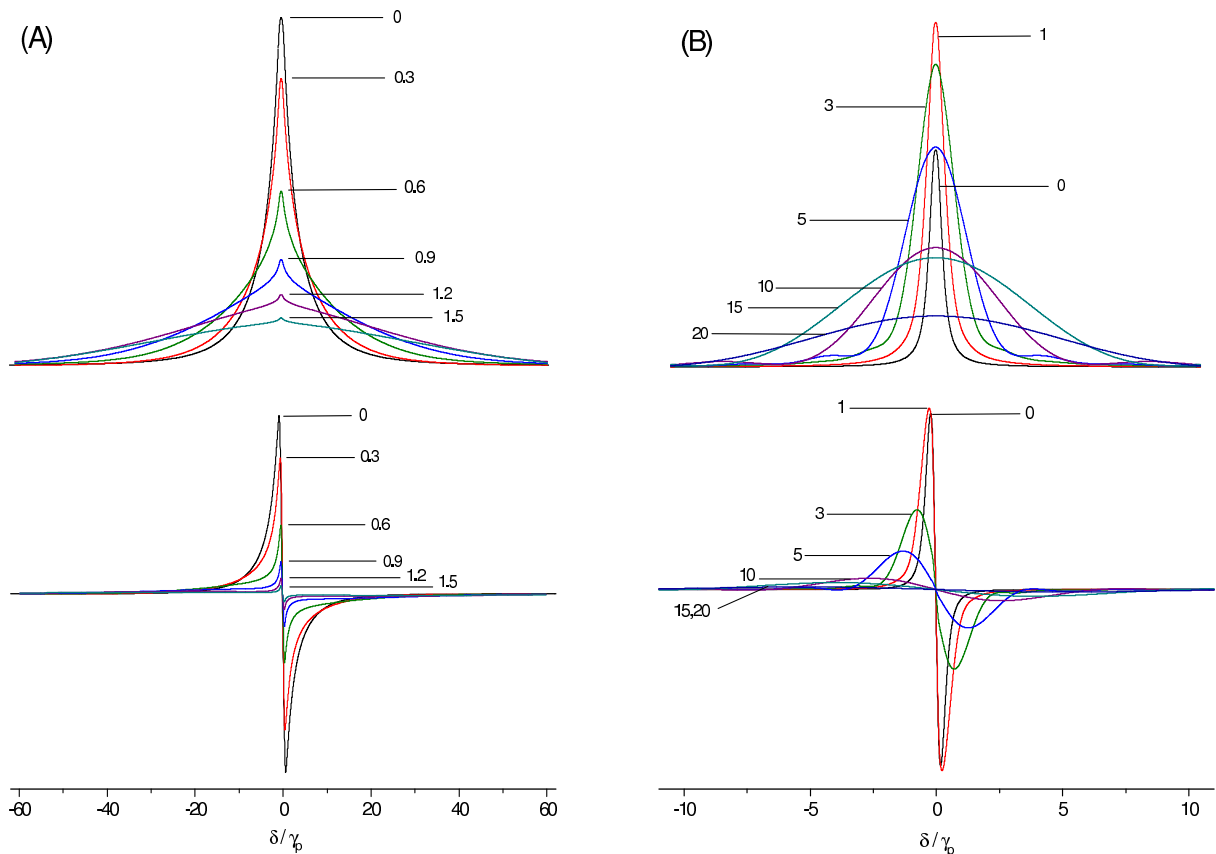


FIG. 9: (Color online) Dark resonance spectra (top) and their derivative (bottom) for A) $\phi = 0.1$ and B) $\phi = 10$ corresponding to different values of the laser detuning $\frac{\delta\omega}{\Gamma}$ from the optical resonance.

more efficient at resonance; such an effect does not exist for a closed system).

III. INFLUENCE OF THE VELOCITY DISTRIBUTION.

Most of the results presented in the preceding sections crucially depend on the assumption that the velocity distribution is a M-B function. For a thin cell, the atomic mean free path in free space exceeds the distance between walls, so that the bulk v_z distribution should be strongly connected to the v_z distribution for the particles at desorption.

A M-B distribution is theoretically predicted for the velocities of particles desorbed from a plane surface, when the surface and the gas are in thermodynamical equilibrium [31]. From the flux of desorbing atoms, one expects to recover a M-B velocity distribution, implying a $\cos\theta$ law (Lambertian law) of probability for the velocity at a given angle θ with respect to the perpendicular to the desorption surface. Interestingly, this standard assumption has been addressed experimentally only seldomly. Experimental data exist from an accurate linear absorp-

tion experiment [32], where a thermodynamical equilibrium between atoms and surface was expected, and from experiments using molecular beams scattered by planar surfaces [33]. In this last case, the distribution is usually referred as Knudsen law, as no thermodynamical equilibrium exists between the incoming particles and the surface.

According to Fig. 8.B the velocities contributing to the dark resonance spectrum in micro-metric thin cells are much smaller than the optically selected velocity $\frac{\Gamma}{k}$, and are currently well below $0.1\frac{\Gamma}{k}$. For alkali atoms, such as Rb or Cs, this corresponds to longitudinal velocities smaller than $v_z = 1 \text{ m/s}$. The existence of such slow atoms, necessarily assumed when considering a M-B distribution, is questionable. For example, even minor effects of surface roughness or imperfections in the wall planarity (i.e. deviation between the local normal direction, and the global one) may prohibit the observation of very small velocities at desorption. In addition, at the limit of very slow velocities, the quantized atomic motion, and the Heisenberg uncertainty casts a limit to the minimal velocity if the atomic position is approximately known. In all these cases, and even if collisional redistribution may allow atoms with nearly null v_z velocity between the walls, the transient evolution of the atomic

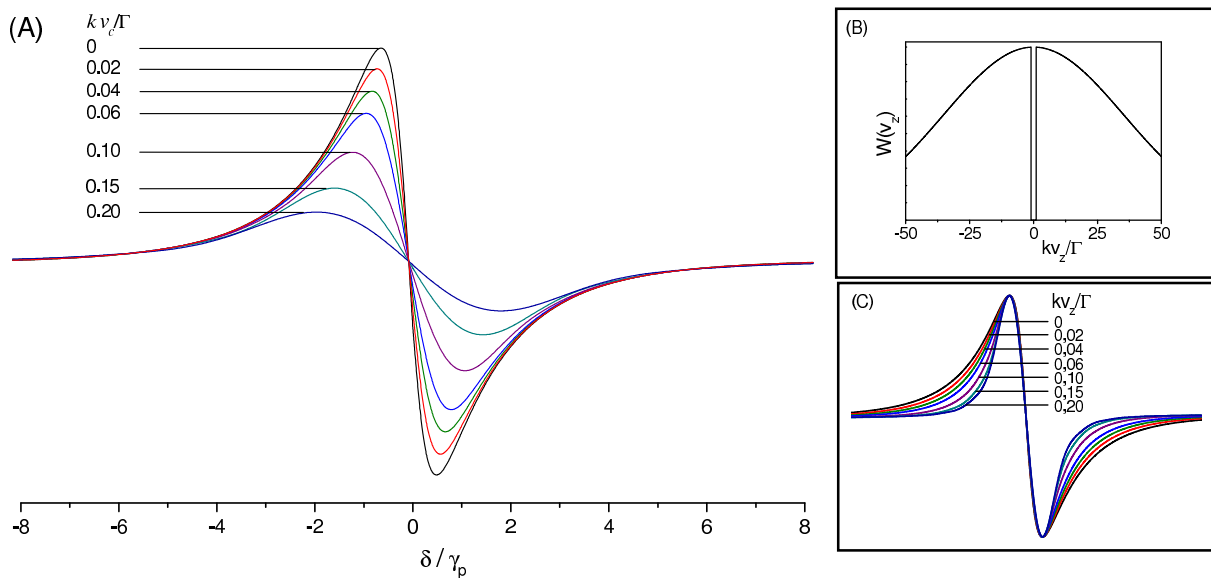


FIG. 10: (Color online) A) Evolution of the derivative of the dark resonance spectrum, peak-to-peak width and amplitude when velocities $|v_z|$ smaller than $\frac{kv_c}{\Gamma}$ are removed from the M-B velocity distribution; as illustrated in B) for $\frac{kv_c}{\Gamma} = 1$. The spectra were calculated for realistic parameters easily attainable in experiments ($kL = 40$, $\Omega = 0.1\Gamma$ ($\phi = 0.4$), $\gamma = 0.001\Gamma$ and $\alpha = 0.7$). For the purpose of lineshapes comparison, in C) the curves are shown normalized to have the same peak-to-peak amplitude and width.

state can no longer be described by a wall-to-wall trajectory. Moreover, atoms leaving the surface at a nearly-grazing incidence undergo a strong van der Waals interaction for a long duration, susceptible to deviate their trajectories. Note that such a possible limitation to the description by a M-B distribution, affecting very slow atoms, could not be addressed in the experiments mentioned above for these extremely small velocities. Similarly, in an atomic scattering experiment, an 80° angle relatively to the normal (i.e. $v_z \simeq 0.2\bar{v}$) is usually an already very large scattering angle. The present results show the importance of the contribution of slow atoms, both in amplitude and for the lineshape. Hence one understands that dark resonances in thin cells may provide a useful tool to investigate the presence of atoms with ultra-slow normal velocities resulting from a desorption process. To analyze this possibility we have studied the modifications of the dark resonance spectrum when the slowest atoms are removed from the velocity distribution. In such case, the narrow structure of the coherent signal at $\delta = 0$ is correspondingly reduced, the spectrum broadens and changes its shape as shown in Fig. 10. In the specific case shown in Fig. 10, obtained for a realistic set of parameters ($\phi = 0.4$, $\gamma = 0.001\Gamma$ has been used corresponding to experiments with Rb or Cs [34]), a significant change in the dark resonance spectrum shape and width is already visible when velocities up to $v_z = 0.1\frac{\Gamma}{k}$ are removed from the velocity distribution. Moreover, the changes resulting from the modified velocity distribution are not limited to a change in amplitude and width, that could be hardly identified if one has no possibility to effectively compare the obtained signal with the one

predicted for a genuine MB distribution. Rather, it is the overall shape of the signal, notably in the ratio between the wings and the behavior at the center, that are modified. Conversely, in purely optical spectroscopy, the contribution of atoms with ultra-slow velocities, although relatively favored in thin cells [10, 35] and depending upon the same ϕ parameter, remains hindered inside the (broad) optical width. Here, the dark resonance scheme introduces extra parameters, finally allowing an RF selectivity in an all-optical measurement. It is also worth noticing that, although going to long cells is apparently favorable to reduce the width, the sensitivity to low velocity atoms is rather obtained for relatively short cells as shown by Fig. 10.

IV. CONCLUSIONS

In summary, we have studied the dark resonances in micro-meter thin cells identifying the relevant physical parameters and discussing the physical mechanisms that determine the shape of the spectra. We have mostly assumed the irradiation to be on resonance with the atomic transition, but we have shown this is not critical (within the optical width). For large values of the parameter ϕ (corresponding to relatively long cells and/or high intensities) narrow dark resonance spectra result from the contribution of all atoms : in spite of the assumption of wall-to-wall trajectory, one hence recovers the results predicted for a macroscopic cell. For small values of ϕ (corresponding to relatively thin micro-metric cells and low intensities), broader dark resonance

spectra are obtained that, nonetheless, should enable an unusual tight velocity selection of ultra-slow atoms. This differs from single laser beam experiments on a two-level transition, for which the predicted enhanced contribution of slow atoms (and according to the same parameter ϕ) remains hindered by the optical width [35]. In our case, it is the EIT scheme that allows to benefit of an RF selectivity in an all-optical measurement. We suggest that dark resonance spectroscopy in thin cells could provide a useful tool for the investigation of the velocity distribution of atoms leaving the surface with grazing trajectories after a desorption process. This possibility, expected from spectroscopy in thin cell [9] (and demonstrated in [36] down to $2m/s$, as compared to the $5m/s$ standard selection associated to the optical width), was until now limited by the optical width of the detection method [10], but turns here to be realistic with the introduction of the arbitrary narrow Raman width as an additional parameter. Other interesting phenomena such as velocity or temperature jumps on a surface [37] or laser induced desorption [33] could also possibly be approached with this technique. The theoretical analysis presented in this work shows a slight dependence on the dark resonance spectral width with the confinement introduced by the thin cell that can notably apply to the consideration of thin cells for the development of compact atomic frequency references [38]. Finally, experiments related to this work are currently underway on Rb or Cs, in which inhomogeneities and/or finite transit time impose a practical lower limit for the dark resonance spectral width. However a spectral width of only $\Delta_{pp} \simeq 200kHz$ have been measured for the hyperfine Raman transition of Rb in a $10\mu m$ thin cell [38].

V. ACKNOWLEDGEMENTS

We would like to thank financial support from ECOS-Sud (contract #U00-E03, France) and CSIC (Uruguay).

VI. APPENDIX: PARAMETERS CHARACTERIZING THE DARK RESONANCE SPECTRA IN A THIN CELL

In this appendix we present the analytic procedure followed to identify the set of parameters ($\frac{\Omega^2 kL}{\Gamma^2}$, $\frac{\delta}{\gamma_p}$, $\frac{\gamma_i}{\gamma_p}$ and α) that characterizes the dark resonance spectra in thin cells.

Defining the real 9-elements vector

$$\sigma = (\sigma_{DD}, \sigma_{CC}, \sigma_{ee}, Re\sigma_{eD}, Im\sigma_{eD}, Re\sigma_{eC}, Im\sigma_{eC}, Re\sigma_{DC}, Im\sigma_{DC},) \quad (4)$$

the Bloch equations (Eq. 1) can be written in the following matrix form

$$\dot{\sigma} = M\sigma + \lambda \quad (5)$$

where $\lambda = (\frac{\gamma}{2} \frac{\gamma}{2} 0 0 0 0 0 0)$. After solving the eigen-values and eigen-vectors problem we have: $M = VDV^{-1}$ where D is the diagonal matrix of eigen-values ϵ_i and V is a transformation matrix (that in particular is not dependent on z due to the symmetry of the system of Fig. 1.A), the spatial integral in Eq. 2 can be written

$$\begin{aligned} & m.V \left(\int_0^{kL} \exp\left(\frac{Dkz}{kv_z}\right) dkz \right) V^{-1}\sigma_o \\ & + m.V \left(\int_0^{kL} \left(\exp\left(\frac{Dkz}{kv_z}\right) - I \right) dkz \right) D^{-1}V^{-1}\lambda \end{aligned} \quad (6)$$

where $m = (000000100)$ allows the notation $Im\sigma_{eC} = m.\sigma$. After calculating the spatial integral in Eq. 6, Eq. 2 can be written

$$\begin{aligned} \Delta I \propto & \Omega kL \int_0^{+\infty} W(v_z) dv_z m.V \left[\left(\exp\left(\frac{DkL}{kv_z}\right) - I \right) (DkL)^{-1}V^{-1}\sigma_o \delta_D \right] + \\ & + \Omega^3 kL^2 \int_0^{+\infty} W(v_z) dv_z m.V \left[\left(\exp\left(\frac{DkL}{kv_z}\right) - I \right) (DkL)^{-1}kv_z - I \right] (DkL)^{-1}V^{-1}\frac{\lambda}{\Omega^2} \end{aligned} \quad (7)$$

We have solved the problem of finding the analytic expression of most of the eigen-values of M by a perturbation procedure on Ω and δ , considering then $\delta \ll \Gamma$ and $\Omega \ll \Gamma$. The matrix M of Eq. (5) have eigen-values around $\frac{-\Gamma}{2}$ and $-\Gamma$ associated to a fast optical evolution

at rates $\frac{\Gamma}{2}$ and Γ and eigen-values around zero, associated to a slow evolution related to the Raman coherence evolution. The dark resonance spectra are essentially determined by the rates of these last eigen-values that have

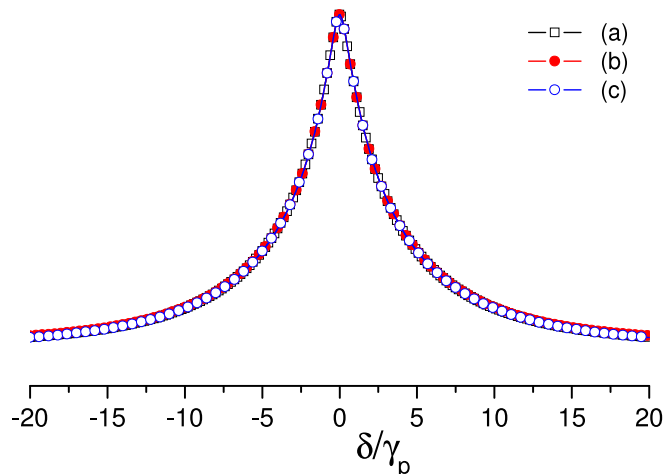


FIG. 11: (Color online) Numerically calculated dark resonance spectra from Eq. (7) for $\phi = 0.1$, $\frac{\gamma}{\gamma_p} = 0.01$ and $\alpha = 0.7$ corresponding to (a) $kL = 1000$, $\Omega = 0.01\Gamma$, $\gamma = 1 \times 10^{-6}\Gamma$ (b) $kL = 250$, $\Omega = 0.02\Gamma$, $\gamma = 4 \times 10^{-6}\Gamma$ and (c) $kL = 25000$, $\Omega = 0.002\Gamma$, $\gamma = 4 \times 10^{-8}\Gamma$. The same vertical scale is used to show all spectra.

a general expression, after the perturbative calculation,

$$\epsilon_i \approx a_i + b_i \Omega^2 + c_i \left(\frac{\delta}{\Omega} \right)^2 \quad (8)$$

for $\delta \ll \Omega$. The constant a_i is equal to $-\gamma$ or $\frac{-\gamma}{2}$ and the constants b_i and c_i depend only on the parameter α . Introducing (8) in the expression DkL we found for each term of the diagonal of D the generic form,

$$\epsilon_i kL = \left(\frac{\Omega^2 kL}{\Gamma^2} \right) \left(\frac{a_i}{\gamma_p} + b_i + c_i \left(\frac{\delta}{\gamma_p} \right)^2 \right) \quad (9)$$

After (9) the exponents in (7) depend on the parameters $\frac{\gamma_p kL}{\Gamma}$, $\frac{\delta}{\gamma_p}$, $\frac{\gamma}{\gamma_p}$ and α , suggesting a dimensionless set of parameters that could determine the dark resonance spectra. We have verified by solving numerically the Eq. 7 that these parameters effectively characterize the dark resonance spectra [see Fig. 11].

-
- [1] E. Arimondo, *Physical Review A* **54**, 2216 (1996).
[2] F. Renzoni and E. Arimondo, *Physical Review A* **58**, 4717 (1998).
[3] S. Brandt, A. Nagel, R. Wynands, and D. Meschede, *Physical Review A* **56**, R1063 (1997).
[4] M. Merimaa, T. Lindvall, I. Tittonen, and E. Ikonen, *Journal of the Optical Society of America B* **20**, 273 (2003).
[5] R. Lutwak, D. Emmons, T. English, W. Riley, A. Duwel, M. Varghese, D. Serkland, and G. Peake, *Proc. 34th Ann. Prec. Time and Time Interv. Sys. App. Meeting*, San Diego, California (2003).
[6] S. Knappe, L. Hollberg, and J. Kitching, *Optics Letters* **29**, 388 (2004).
[7] P. Schwindt, S. Knappe, V. Shah, L. Hollberg, and J. Kitching, *Applied Physics Letters* **85**, 6409 (2004).
[8] J. Vanier and C. Audoin, *Quantum Physics of Atomic Frequency Standards* (Adam Hilger, 1989), ISBN 0-85274-434-X.
[9] S. Briaudeau, D. Bloch, and M. Ducloy, *Europhysics Letters* **35**, 337 (1996).
[10] S. Briaudeau, D. Bloch, and M. Ducloy, *Physical Review A* **59**, 3723 (1999).
[11] S. Briaudeau, S. Satiel, G. Nienhuis, D. Bloch, and M. Ducloy, *Physical Review A* **57**, R3169 (1998).
[12] G. Dutier, Yarovitski, S. Satiel, A. Papoyan, D. Sarkisyan, D. Bloch, and M. Ducloy, *Europhysics Letters* **63**, 35 (2003).
[13] M. Fichet, G. Dutier, A. Yarovitski, P. Todorov, I. Hamdi, I. Maurin, S. Satiel, D. Sarkisyan, M.-P. Gorza, D. Bloch, et al., *Europhysics Letters* **77**, 54001 (2007).
[14] K. Fukuda, M. Kinoshita, A. Hasegawa, M. Tachikawa, and M. Hosokawa, *Journal of the National Institute of Information and Communications Technology, Japan* **50**, 95 (2003).
[15] H. Failache, A. Lezama, D. Bloch, and M. Ducloy, *Europhysics Conference Abstracts* **28F**, 2 (2004).
[16] T. Varzhapetyan, D. Sarkisyan, L. Petrov, C. Andreeva, D. Slavov, S. Satiel, A. Markovski, G. Todorov, and S. Cartaleva, *Proc. SPIE* **5830**, 196 (2005).
[17] A. Sargsyan, D. Sarkisyan, and A. Papoyan, *Physical Review A* **73**, 033803 (2006).
[18] A. Izmailov, *Optics and Spectroscopy* **80**, 321 (1996).
[19] H. Tajalli, S. Ahmadi, and A. C. Izmailov, *Laser Physics* **8**, 1223 (1998).

- [20] A. Namdar, H. Tajalli, M. Kalafi, and A. C. Izmailov, *Laser Physics* **9**, 476 (1999).
- [21] D. Petrosyan and Y. P. Malakyan, *Physical Review A* **61**, 053820 (2000).
- [22] F. Renzoni, A. Lindner, and E. Arimondo, *Physical Review A* **60**, 450 (1999).
- [23] Y. Dancheva, G. Alzetta, S. Cartaleva, M. Taslakov, and C. Andreeva, *Optics Communications* **178**, 103 (2000).
- [24] P. Valente, H. Failache, and A. Lezama, *Physical Review A* **65**, 023814 (2002).
- [25] A. Aspect, E. Arimondo, R. Kaiser, N. Vansteenkiste, and C. Cohen-Tannoudji, *Physical Review Letter* **61**, 826 (1988).
- [26] A. Aspect, E. Arimondo, R. Kaiser, N. Vansteenkiste, and C. Cohen-Tannoudji, *Journal of the Optical Society of America* **B 6**, 2112 (1989).
- [27] B. Zambon and G. Nienhuis, *Optics Communications* **143**, 308 (1997).
- [28] G. Dutier, S. Saltiel, D. Bloch, and M. Ducloy, *Journal of the Optical Society of America* **B 20**, 793 (2003).
- [29] M. Schuurmans, *Le Journal de Physique* **37**, 469 (1976).
- [30] T. A. Vartanyan and D. L. Lin, *Physical Review A* **51**, 1959 (1995).
- [31] W. Gaede, *Annalen der Physik* **41**, 331 (1913).
- [32] D. Grischkowsky, *Applied Physics Letters* **36**, 711 (1980).
- [33] V. G. Bordo and H.-G. Rubahn, *Physical Review A* **60**, 1538 (1999).
- [34] E. Figueroa, F. Vewinger, J. Appel, and A. I. Lvovsky, *Optics Letters* **31**, 2625 (2006).
- [35] S. Briaudeau, Ph.D. thesis, Université Paris-Nord (1998), unpublished. It is shown that in a purely optical experiment, removing the slow atoms apparently implies a reduction of the signal width, and a broadening of the transition. However, the overall shape remains similar, and this makes it difficult to attribute a given width to an effect of the velocity distribution, or to a different cause for broadening such as regular interatomic collisions.
- [36] S. Briaudeau, S. Saltiel, J. Leite, M. Oria, A. Bramati, A. Weis, D. Bloch, and M. Ducloy, *Journal de Physique IV France* **10**, Pr.8, 145 (2000).
- [37] F. Goodman and H. Wachman, *Dynamics of Gas-Surface Scattering* (Academic Press, New York, 1976).
- [38] H. Failache, L. Lenci, and A. Lezama, CLEO/QELS, Baltimore, Maryland, USA (2007).